

**DIVINER CONSTRAINTS ON PLAGIOCLASE COMPOSITIONS AS OBSERVED BY THE SPECTRAL PROFILER AND MOON MINERALOGY MAPPER.** M. B. Wyatt<sup>1</sup>, K. L. Donaldson Hanna<sup>1</sup>, C. M. Pieters<sup>1</sup>, J. Helbert<sup>2</sup>, A. Maturilli<sup>2</sup>, B. T. Greenhagen<sup>3</sup>, D. A. Paige<sup>3</sup>, and P. G. Lucey<sup>4</sup>, <sup>1</sup>Brown University, Department of Geological Sciences, Box 1846, Providence, RI 02912 (michael\_wyatt@brown.edu), <sup>2</sup>Institute for Planetary Research, German Aerospace Center DLR, Rutherfordstr. 2, Berlin-Adlershof, Germany, <sup>3</sup>University of California, Los Angeles, Department of Earth and Space Sciences, 595 Charles Young Drive East, Los Angeles, CA 90095, <sup>4</sup>University of Hawaii, Institute for Geophysics and Planetology, 1680 East-West Road, Honolulu, HI 96822.

**Introduction:** Near-infrared observations from the SELENE Spectral Profiler (SP) have been used to identify iron-bearing crystalline plagioclase in the central peaks of several large highland craters [1]. Recent image-cube data from the Chandrayaan-1 Moon Mineralogy Mapper (M<sup>3</sup>) acquired across the Orientale Basin have also been used to identify iron-bearing crystalline plagioclase [2]. These observations are significant because they validate the near-infrared identification of plagioclase on the Moon.

Shocked plagioclase had been previously inferred from a lack of Fe<sup>2+</sup> absorptions [3-5] in near-infrared measurements of high albedo locations as plagioclase can become sufficiently disordered with shock to lose its absorption bands [6]. The identification of iron-bearing crystalline plagioclase in the near-infrared comes from a broad absorption band at ~ 1.3 μm due to electronic transitions of Fe<sup>2+</sup>. Near-infrared laboratory studies of this feature have suggested its band depth and center position may vary with Fe and An content respectively [7-9].

**DIVINER:** The upcoming Diviner Lunar Radiometer Experiment (DLRE) on the Lunar Reconnaissance Orbiter (LRO) will provide the first global coverage maps of thermal-infrared derived compositions on the Moon. Extensive thermal-infrared laboratory studies of plagioclase minerals and plagioclase-rich rocks indicate that both plagioclase abundances and compositions can be determined by linear deconvolution of mixed spectra [10-11]. However, Diviner has only three mineralogy spectral channels centered at 7.8, 8.2, and 8.6 μm, so it is important to investigate the applicability of Diviner data for plagioclase composition studies.

In this study, we review thermal-infrared laboratory spectra of mineral endmembers, a mineral mixture, Apollo highlands, and Apollo mare soil samples convolved to Diviner spectral bands [12] and focus on the ability of Diviner data to distinguish plagioclase compositions.

**Samples and Methods:** Laboratory emissivity spectra of < 25 μm and > 90 μm grain size fractions of plagioclase, low- and high-Ca pyroxenes, olivine, and ilmenite used in this work are from the Berlin emissivity database (BED) [13]. A 50/50 wt% mineral

mixture of endmembers anorthite and olivine is also examined.

Lunar soil samples are characterized by the Lunar Soil Characterization Consortium (LSCC) [14-15]. Apollo mare soil samples chosen for this study include 10084, 12001, 12030, 15041, 15071, 71061, 71501, 70181, and 79221 [14] and Apollo 16 highlands soil samples include 61141, 61221, 62331, 64801, 67471, and 67481 [15]. Apollo lunar soils are plotted in Figure 1 on a plagioclase-orthopyroxene-clinopyroxene ternary diagram [16]. Brown University's RELAB FTIR spectrometer was used to measure thermal-infrared spectra of each lunar soil sample for the 10 – 20 μm grain size fraction [17]. Thermal-infrared RELAB spectra are converted to emissivity using the approximation to Kirchoff's relation E=1-R. All thermal-infrared spectra are convolved to Diviner's three spectral bands using ENVI's spectral resampling tool.

The Diviner spectral bands were chosen specifically to measure the location of the Christiansen Feature (CF). The CF is an emission maximum, or reflectance minimum, first described as an indicator of compositions by [18]. The CF shift to shorter wavelengths for particulate materials in a vacuum environment is well constrained [19-20]. In this study, we calculate band ratios for each spectrum, assume that the CF shift applied to each spectral band is the same, and apply the ratios to accurately identify lunar compositions.

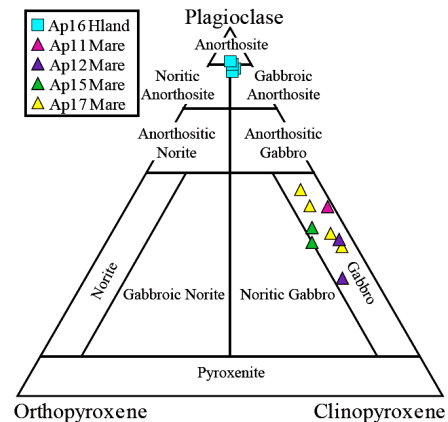


**Figure 1.** Highland soils are classified as anorthosite and mare as gabbro. It is important to note that anorthosite soils are not pure plagioclase, but contain small abundances of mixed pyroxenes (~ 4-10 total vol. %).

**Thermal-Infrared Data:** Recent work by [12] explored how to use Diviner band ratios for distinguishing fine-grained ( $< 25 \mu\text{m}$ ) minerals, mineral mixtures and lunar soil samples. Figure 2 shows the 7.8/8.6 versus 8.6/8.2 Diviner band ratios for plagioclase, orthopyroxene, clinopyroxene, olivine, ilmenite, a 50/50 wt% plagioclase-olivine mixture, and lunar soil spectra [12]. Each mineral group is clearly distinguished using the 8.6/8.2 ratio with plagioclase plotting in the upper left (CF at shorter wavelengths) and olivine plotting in the lower right (CF at longer wavelengths). Mixture endmembers anorthite and olivine plot within their respective mineral groups, however the 50/50 mixture is indistinguishable from orthopyroxene and clinopyroxene. Work by [12] demonstrated that integrating Diviner thermal-infrared data with near-infrared spectral parameters (e.g. spectral curvature, integrated band depth, and band depth position) resolves these mineral mixture uncertainties. The Apollo highlands spectra plot closer to the plagioclase mineral group compared to Apollo mare spectra, consistent with its classification of anorthosite.

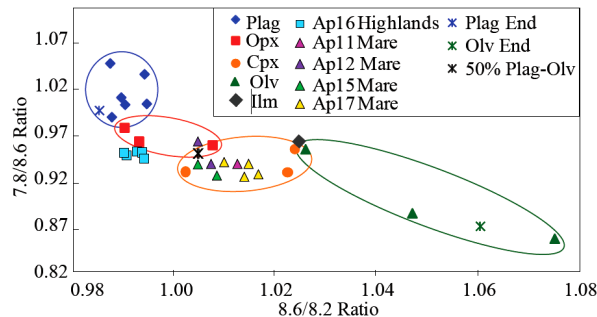


**Figure 2.** Simple band ratios 7.8/8.6 and 8.6/8.6 plotted against one another for individual minerals, a mixture of minerals, and lunar soils.

**Plagioclase Focused Studies:** The regions where crystalline plagioclase have been identified with SP and  $M^3$  data are ideal locations on the Moon for Diviner data analysis. We now investigate the utility of Diviner data to distinguish different plagioclase compositions. It should be noted that this analysis is only applicable to the pure plagioclase regions on the Moon.

Figure 3 (top) shows a 7.8/8.6 ratio versus 7.8/8.2 ratio for coarse- ( $> 90 \mu\text{m}$ ) and fine-grained ( $< 25 \mu\text{m}$ ) plagioclase endmembers. The coarse- and fine-grained fields are distinguished due to the unique position and shape of the CF for each mineral composition. The middle and bottom sections of Figure 3 separate the coarse- and fine-grained fields to maximize the differences between each plagioclase composition. The 7.8/8.6 ratio versus 7.8/8.2 ratio clearly sets apart the plagioclase series with the Ca-rich anorthite plotting

on the left and the Na-rich albite and oligoclase plotting on the right for both particle sizes. Intermediate compositions plot in the middle.

While it is not possible to determine the An # with these ratios, it is possible to distinguish Ca-rich, intermediate, and Na-rich compositions. This will be significant for constraining plagioclase compositions in the feldspathic highlands, specifically the distributions of ferroan anorthosite and alkali-suite materials.

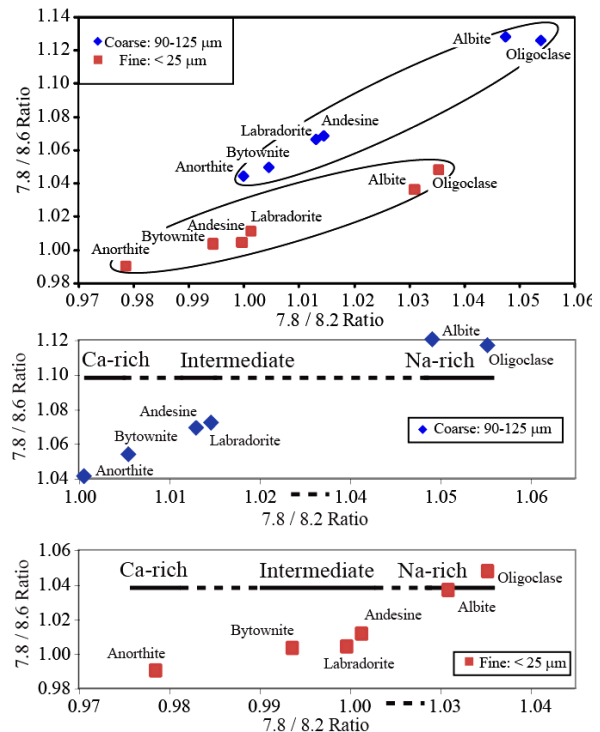


**Figure 3.** Simple band ratios 7.8/8.6 and 7.8/8.2 plotted against one another for plagioclase minerals.

**References:** [1] Matsunaga T. et al. (2008) *GRL*, 35, L23201. [2] Pieters C. et al. (2009) *LPSC XL*, Abstract #2052. [3] Spudis P. et al. (1984) *JGR*, 89, C197-C210. [4] Hawke B. R. et al. (2003) *JGR*, 108, (E6). [5] Tompkins S. and Pieters C. (1999) *Met. & Planet. Sci.*, 34, 25–41. [6] Johnson J. and Horz F. (2003) *JGR*, 108, 5120. [7] Adams J. B. and McCord T. B. (1971) *PLPSC* 3, 2183–2195. [8] Bell P. M. and Mao H. K. (1973) *GCA*, 37, 755–759. [9] Cheek L. C. et al. (2009) *LPSC XL*, Abstract #1928. [10] Ruff S. W. (1998) *Ph.D. dis. ASU*. [11] Milam K. et al. (2004) *JGR*, 109, 4001. [12] Donaldson Hanna K. L. et al. (2009) *LPSC XL*, Abstract # 2286. [13] Maturilli A. et al. (2008) *Planet. & Space Sci.*, 56, 420–425. [14] Taylor L. et al. (2001) *Met. & Planet. Sci.*, 36, 285–299. [15] Taylor L. et al. (2003) *LPSC XXXIV*, Abstract #1774. [16] Stöffler D. et al. (1980) In *Proc. Conf. Lunar High. Crust*, 51–70. [17] Pieters C. and Hiroi T. (2004) *LPS XXXV*, Abstract #1720. [18] Conel J. (1969) *JGR*, 74, 1614–1634. [19] Logan L. M. et al. (1973) *JGR*, 78, 4983–5003. [20] Salisbury J. and Walter L. (1989) *JGR*, 94, 9192–9202.